Tryptophan Hydrogen Bonding and Electric Dipole Moments: Functional Roles in the Gramicidin Channel and Implications for Membrane Proteins†

W. Hu‡ and T. A. Cross*

Center for Interdisciplinary Magnetic Resonance at the National High Magnetic Field Laboratory, Institute of Molecular Biophysics, and Department of Chemistry, Florida State University, Tallahassee, Florida 32306

Received July 17, 1995; Revised Manuscript Received September 8, 1995®

ABSTRACT: The known high-resolution structure and dynamics characterization of the lipid bilayer-bound polypeptide gramicidin A provides a unique opportunity to study structure−function and dynamics−function correlations in a model membrane protein. In particular, the indoles have a variety of very important functional roles in this cation channel that will undoubtedly be recognized in membrane proteins. That indoles and phenols are oriented at the hydrophobic−hydrophilic interface of lipid bilayers is already well-recognized in membrane proteins. The most buried indole of the gramicidin channel, Trp_9, is shown by ^{15}N solid state NMR to be exposed to the hydrophilic surface through hydrogen exchange. Here the importance of the indole dipole moments is described for cation conductance. Preparation of samples with high concentrations of Na^+ is shown by high-resolution orientational constraints derived from ^2H NMR to have no structural effect on the indole side chain conformations. These dipoles stabilize cations in the binding sites near the channel entrance and substantially reduce the potential energy barrier at the bilayer center. This latter finding conclusively documents that the rate-limiting step in cation conductance by this channel involves the barrier at the bilayer center. Furthermore, dynamics of the indole rings cause significant fluctuations in the energy of stabilization at the binding site that may result in a rapid mechanism for gating the channel.

Understanding the molecular basis of function is one of the primary pursuits of structural biology. Often, model systems are used to gain insights into complicated systems that go beyond the reach of current methodology and technology. High-resolution structural and dynamic information is very difficult to obtain for membrane proteins. The gramicidin channel is currently the highest resolution structure of a polypeptide or protein that has been solved in a hydrated lipid environment (Ketchem et al., 1993). This report takes advantage of such knowledge to analyze the indole dipole moments and their influence on cation conductance.

The occurrence of tryptophan in membrane proteins is much higher than in water soluble proteins (Schiffer et al., 1992). These residues for the few proteins that are structurally characterized are almost exclusively located in the hydrophilic−hydrophobic interface (Michel & Deisenhofer, 1990; Henderson et al., 1990; Meers, 1990; Chattopadhyay & McNamee, 1991; Schiffer et al., 1992; Hu et al., 1993). Furthermore, these residues are spatially oriented with the six-membered ring into the hydrophobic domain, and the indole N−H is aligned so as to hydrogen bond to the surface. This suggests that the indoles play an important role in orienting membrane proteins with respect to this heterogeneous and anisotropic environment (Schiffer et al., 1992).

Gramicidin is a polypeptide of 15 amino acids having the following sequence: HCO-Val_1-Gly_2-Ala_3-D-Leu_4-Ala_5-D-Val_6-Val_7-D-Val_8-Trp_9-D-Leu_{10}-Trp_{11}-D-Leu_{12}-Trp_{13}-D-Leu_{14}-Trp_{15}-$NHCH_2CH_2OH$. As a dimer, it forms a single-stranded helix with 6.3 residues in a right-handed helix. The backbone structure has been solved by solid state NMR (Ketchem et al., 1993), and the indole orientations have been refined (Hu et al., 1995). The helix and channel pore are arranged parallel to the bilayer normal. The interactions between gramicidin and lipid are not well-defined, but there have been numerous suggestions in the literature that the tryptophans of gramicidin may hydrogen bond to the lipids (Meulendijks et al., 1989; O'Connell et al., 1990; Scarlatta, 1991; Lazo et al., 1992; Hu et al., 1993); while the results of these studies are suggestive, there remain no definitive experimental or computational results. The interactions in the hydrocarbon domain appear to be weak. A dynamic phase boundary has been described between the lipid and peptide (Lee et al., 1995). While there is a well-defined gradient in fatty acyl dynamics from the ester linkage to the bilayer center, there appears to be no such dynamics gradient for the side chains of the polypeptide from the bilayer surface to the bilayer center. The tryptophans in the gramicidin cation channel have several roles. Not only do they orient the channel with respect to the lipid bilayer (Hu et al., 1993), but they stabilize the channel conformation versus other double helical conformations in this environment (O'Connell et al., 1990; Van Mau et al., 1994; Seoh & Busath, 1995; Arumugam et al., 1995); they are required for the modulation effect of gramicidin on lipid phases (Killian, 1992), and they facilitate cation conductance (Becker et al., 1991). While it has been known for decades that gramicidin forms a monovalent cation-selective channel, the details of how this channel facilitates cation conductance is not well-known.

Very extensive studies have been performed with single channel conductance measurements (Daumas et al., 1991; Becker et al., 1991; Busath, 1993) that have led to detailed kinetic models of cation conductance (Becker et al., 1992).

† This work has been supported by the National Institutes of Health (AI-23007) and the National High Magnetic Field Laboratory.

‡ Present address: Biophysics Research Division, University of Michigan, 930 North University, Ann Arbor, MI 48109-1055.

® Abstract published in *Advance ACS Abstracts,* October 15, 1995.

0006-2960/95/0434-14147$09.00/0

The three-barrier, two-binding site model has been widely adopted (Benamar et al., 1993; Van Mau et al., 1994). So, the potential energy profile is considered to have two minima for these two binding sites and three maxima, with the largest barrier occurring at the bilayer center. The other maxima are associated with the channel entrance and the stripping of water from the primary hydration sphere of the cations. The symmetry of this dimer is broken upon binding one cation (strong binding site), causing the unfilled site to become a weak binding site. The binding constants of many different monovalent and divalent cations to both the strong and weak binding sites in the channel have been determined (Hladky et al., 1979; Urry et al., 1982, 1989; Hinton et al., 1988).

It has been recognized for many years that, in substituting for tryptophan with amino acids having different dipole moments, changes in the conductance of the channel occur. However, without structural information as to how these dipole moments are oriented with respect to the channel axis, the exact role of the dipole in the conductance process has not been quantifiable. The simplest substitutions, in which phenylalanine has been substituted for tryptophan, incrementally remove the dipole moments from the channel (Tredgold et al., 1977; Van Mau et al., 1988; Becker et al., 1991). It was noted in this latter study that the conductance was incrementally decreased as one, two, or three indoles were removed from the polypeptide sequence. The authors suggested, on the basis of these conductance observations, that each of the indoles would have approximately the same orientation.

For other amino acid substitutions, the interpretation has been very difficult because of the multiple functional roles for the indoles. For instance, when tyrosine is substituted, it is not clear how the hydrogen bonding to the bilayer surface and the electric dipole moment effect on conductance are compromised. In other words, there will be a change in the hydrogen bond-donating geometry with respect to the bilayer surface, as well as in the dipole moment orientation with respect to the molecular frame of the side chain and with respect to the channel.

Solid state NMR is used here to study gramicidin in an anisotropic environment. Combined with the use of uniformly aligned samples, high-resolution structural and dynamic constraints can be obtained (Cross, 1994; Cross & Opella, 1994; Koeppe et al., 1994; Separovic et al., 1991). Previously (Hu et al., 1993; Ketchem et al., 1993; Koeppe et al., 1994), a number of possible conformations that were consistent with the NMR constraints have been identified. In the accompanying paper (Hu et al., 1995), a unique assignment for the resonances of Trp_9 has been achieved, and with this, a unique orientation of this indole with respect to the bilayer normal. This single orientation for each indole with respect to B_o is consistent with four possible pairs of torsion angles. These correspond to just two possible rotameric states on the χ_1/χ_2 conformational map. From functional and energetic considerations, a most probable indole conformation is achieved for each of the tryptophan side chains. From these indole orientations, a detailed analysis of the dipole moment influence on channel conductance is achieved. Furthermore, solid state NMR of oriented samples is used to study solvent accessibility to the indole rings and to study the influence of cation binding in the channel on the tryptophan conformations.

METHODS AND MATERIALS

Sample preparation was described in the accompanying paper (Hu et al., 1995). The ^{15}N NMR spectra were obtained on two spectrometers; one was assembled around an Oxford Instruments 400/89 superconducting magnet and a Chemagnetics data acquisition system, and the other is an IBM/Bruker WP200 instrument with a heavily modified solids accessory. Cross-polarization with ^1H dipolar decoupling was used for all ^{15}N spectra with typical parameters of 6 μs 90° pulse widths, 1 ms mixing time, and a 7 s recycle delay. The two-dimensional separated local field (SLF)[1] spectrum was obtained at 40.6 MHz using 16 t_1 increments of 20 μs and without homonuclear decoupling and hence without scaling the dipolar dimension. The ^2H dipolar-coupled ^{15}N spectrum was obtained at 20.3 MHz as a standard one-dimensional chemical shift spectrum. ^2H NMR spectra were obtained at 61.5 MHz using the standard quadrupole echo pulse sequence. Typical parameters for data acquisition included a 1 MHz sweep width, 2.8 μs 90° pulse width, 30 μs echo delays, and a 0.5 s recycle delay.

RESULTS

The orientational constraints from the previous paper (Hu et al., 1995) have resulted in the definition of a unique orientation for each indole ring with respect to the lipid bilayer. However, there are four possible χ_1/χ_2 torsion angle pairs for each tryptophan that can achieve these indole ring orientations, as shown in Figure 1. The torsion angles have been defined using the most recent refinement of the channel backbone structure (Ketchem et al., 1993) which precisely constrains the $C_\alpha-C_\beta$ axis orientation and position with respect to the channel and lipid bilayer. Two of the conformations for Trp_9, IA and IIA, differ in χ_2 by 51°; i.e., they are in the same rotameric state. Similarly, IB and IIB differ in χ_2 by 51° and are also in the same rotameric state. Figure 1 is drawn to show the symmetry between IA and IB and between IIA and IIB. In each case, the symmetry plane is defined by the $C_\alpha-C_\beta$ axis and the bilayer normal.

The orientation of the dipole moment within the indole ring is well-characterized (Weiler-Feischenfeld et al., 1970), and in Figure 1, components of the electric dipole moment in the plane of the bilayer for each tryptophan side chain are shown. The magnitudes of the perpendicular components ($\mu_\perp$) have been uniquely defined by the orientational constraints, as have the parallel components ($\mu_{||}$). Here, $\mu_\perp$ is further decomposed into radial (μ_R) and tangential (μ_T) components in the plane of the bilayer that differ in magnitude and sign for each torsional solution set. It is known that the indoles of the gramicidin channel help to stabilize cations in their binding site near the bilayer surface and adjacent to the indole rings (Becker et al., 1992). Therefore, μ_R should be oriented such that the negative end of the moment is directed toward the cation on the channel axis. The orientation of the radial component for conformers IIA and IIB is such that cations would be destabilized, and therefore, conformers IA and IB are favored and not those of IIA and IIB. This argument is further strengthened by Raman results (Takeuchi et al., 1990) that suggest that the

[1] Abbreviations: SLF, separated local field; SDS, sodium dodecyl sulfate.

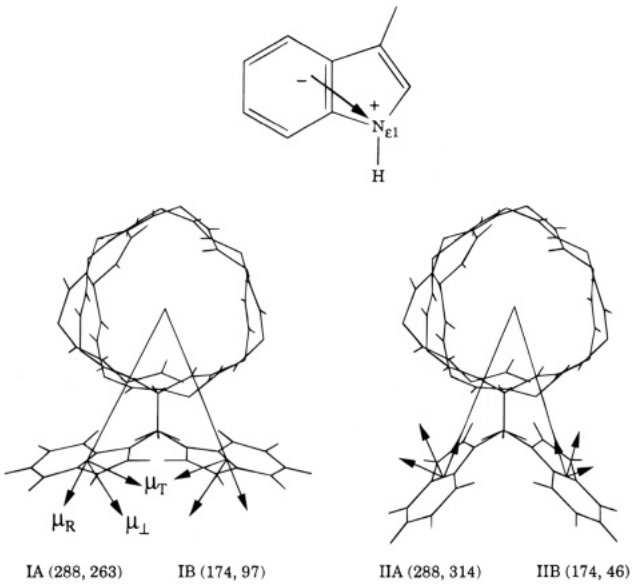

FIGURE 1: Four possible conformers for a given unique orientation of an indole ring (Trp_9) with respect to the bilayer normal and the channel axis. The indole ring at the top displays the fixed orientation of the dipole moment with respect to the molecular frame. At the bottom, with two end views of the channel, conformers IA and IIA differ only in the value of χ_2; similarly, conformers IB and IIB differ only in the value of χ_2. The magnitude and direction of the dipole moment is presented as components parallel ($\mu_{||}$ not shown) and perpendicular ($\mu_\perp$) to the channel axis. Furthermore, the perpendicular component which is in the plane of the bilayer is decomposed into components radial (μ_R) and tangential (μ_T) to the channel axis. Each conformer has distinctly different components. Because the four tryptophans of gramicidin have similar orientations, a similar pattern for the dipole moments is achieved for each tryptophan.

χ_2 angles for the indoles are $\pm 90°$, consistent with both IA and IB, but inconsistent with IIA and IIB.

The reduction in conformational possibilities is true not only for Trp_9 but also for each of the other tryptophans. Based on these results, four remaining combinations of Trp_{15} and Trp_9 are shown in Figure 2. Two of these combinations have severe atomic overlap and are eliminated from consideration (Figure 2A,B). One combination is stabilized by a considerable stacking interaction between these two aromatic rings (Figure 2B). In proteins, 60% of aromatic side chains are involved in stacking interactions that contribute an energy for structural stabilization of 4−8 kJ/mol (Burley & Petsko, 1988). There is also indirect evidence for stacking from the dynamics results reported in the accompanying paper (Hu et al., 1995) and from fluorescence studies (Scarlatta, 1988). Therefore, a most probable conformation for Trp_9 (χ_1/χ_2, 288°/263°) and Trp_{15} (χ_1/χ_2, 302°/264°) can be identified on the basis of the sum of these considerations.

Figure 3 is a schematic view down the channel axis of two possible sets of tryptophan orientations that have the same sign for all of the tangential components. Various computational studies have indicated that it is likely that Na^+ will pass through the channel off-axis, i.e., on a helical path (Skerra & Brickman, 1987; Jordan, 1990; Elber et al., 1995). If cation conductance was on-axis, the tangential component would have an insignificant effect, but if the conductance pathway is off-axis, the tangential component of the dipole could play a significant role in the conductance process. It is suggested here that the tangential components should have

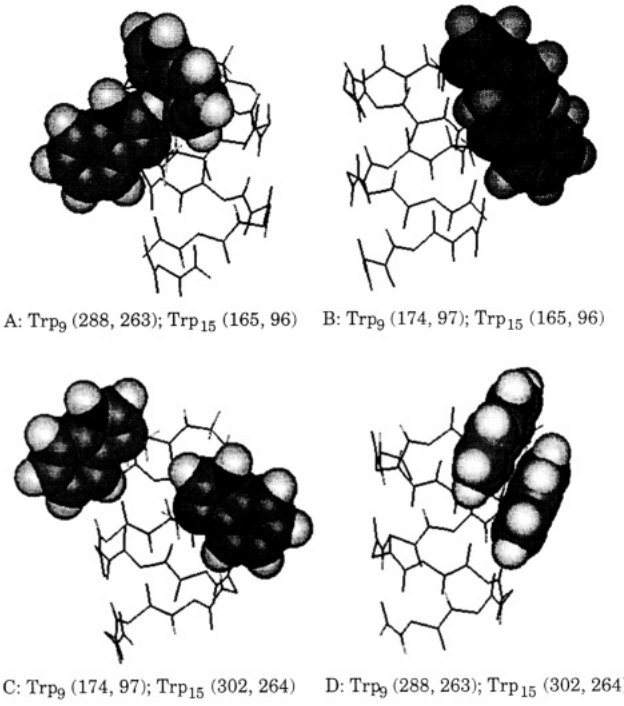

FIGURE 2: Four possible conformer combinations of Trp_9 and Trp_{15} shown with a side view of the gramicidin channel monomer. There are significant van der Waals violations for combinations in parts A and B. The two tryptophans in parts C do not interact, while those in part D are well-positioned for a considerable stacking interaction.

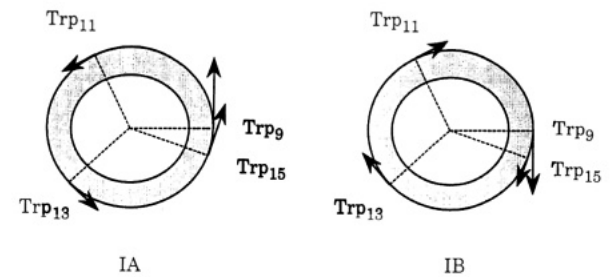

FIGURE 3: There are two conformational combinations for the four tryptophans out of a total of 16 in which the tangential components (μ_T) of the dipole moments have the same tangential direction and hence form a coherent path for facilitating cation transit. The dihedral angles for configuration IA are as follows: Trp_9 (288°/263°), Trp_{11} (290°/279°), Trp_{13} (297°/270°), and Trp_{15} (302°/264°). The angles for configuration IB are as follows: Trp_9 (174°/97°), Trp_{11} (171°/81°), Trp_{13} (169°/90°), and Trp_{15} (165°/96°). Only the IA configurations have Trp_9 and Trp_{15} stacked.

the same sign so as to facilitate cation translation through the channel, i.e., a single direction for the cation. Only one of these combinations (IA) shown in Figure 3 includes the stacked arrangement of Trp_9 and Trp_{15} rings, and therefore, we have established a most probable set of tryptophan conformations for the gramicidin channel which has Trp_{11} $\chi_1 = 290°$ and $\chi_2 = 279°$, as well as Trp_{13} $\chi_1 = 297°$ and $\chi_2 = 270°$.

Figure 4 displays this most probable set of tryptophan ring orientations in both axial and side views. By establishing a most probable conformation, the coordinates of the rings are defined with respect to the channel and the lipid bilayer. And for the purposes of calculating an electrostatic energy between the dipole and cation, the geometry and dipole component magnitudes are now uniquely defined (Table 1). In Figure 5, the important geometric parameters for calculating this energy are illustrated for the Trp_9 ring. Furthermore,

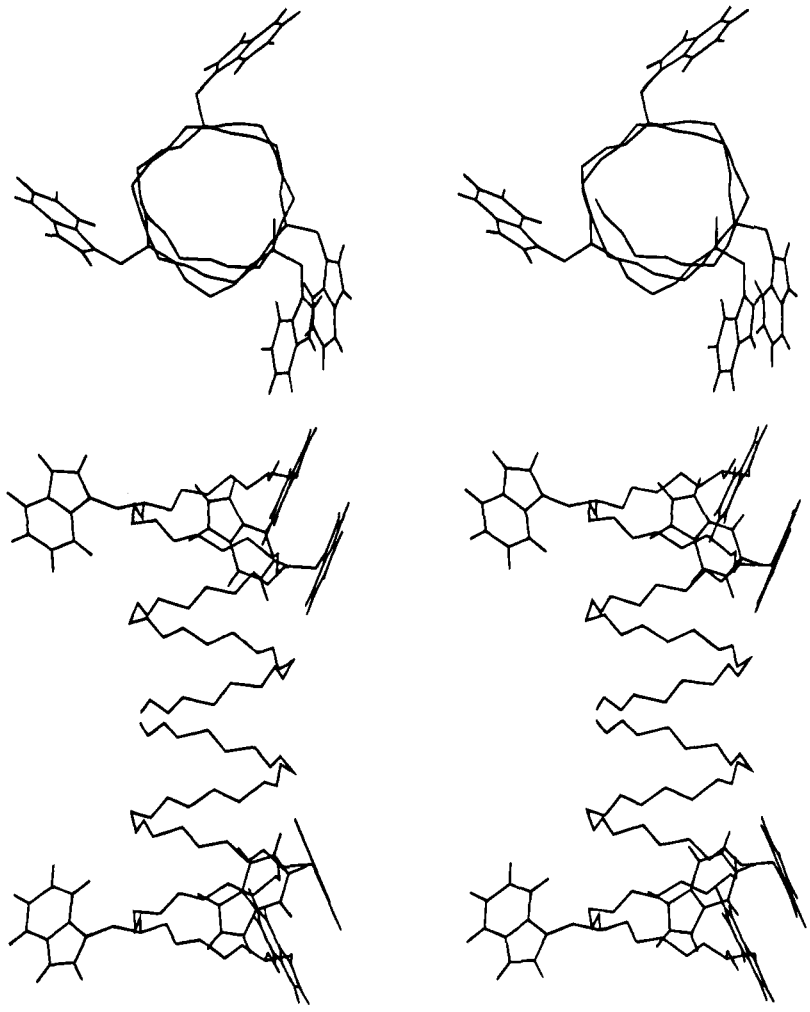

FIGURE 4: End view of a channel monomer and the side view of the channel dimer shown in stereo with the most probable tryptophan conformers. The backbone structure is from the recent refinement (Ketchem et al., 1993), and it is displayed with only the main chain heavy atoms. For clarity, only the indole side chains are shown. The χ_1 and χ_2 dihedral angles are as follows: Trp_9 (288°/263°), Trp_{11} (290°/279°), Trp_{13} (297°/270°), and Trp_{15} (302°/264°).

Table 1: Geometric and Electrostatic Parameters Associated with the Most Probable Tryptophan Conformation

	Trp_9	Trp_{11}	Trp_{13}	Trp_{15}
critical distances (Å)				
d_i	10.7	10.9	12.5	13.6
$d_\perp$	7.4	6.6	7.5	7.7
$N_{\epsilon 1}-H$	10.1	11.2	12.4	13.5
critical orientations (deg)				
d_i	44	37	37	34
$N_{\epsilon 1}-H$	31	32	38	43
μ	25	14	20	24
dipole components (D)				
$\mu_{\parallel}$	1.89	2.02	1.95	1.90
$\mu_\perp$	0.87	0.50	0.72	0.85
μ_R	0.29	0.26	0.57	0.61
μ_T	0.82	0.42	0.43	0.60
μ_i	1.56	1.76	1.91	1.91

the χ_2 dependence of these geometric parameters is shown for the most probable χ_1 value of 288°. At the χ_2 value of 263°, the $N_{\epsilon 1}-H$ hydrogen is shown to have a nearly maximal distance (d_{NH}) from the bilayer center and to be in a near optimal position for hydrogen bonding to the bilayer surface. Most other χ_2 orientations would result in the $N_{\epsilon 1}-H$ being buried more deeply within the hydrophobic domain of the bilayer. The d_i distance, between the dipole and cation monopole on the channel axis at the bilayer center, is less sensitive to χ_2, but it has a minimal value for the most probable conformation which means a maximal electrostatic influence on cation transit across the potential energy barrier at the bilayer center. The $d_\perp$ distance is calculated to the channel axis which is only an approximation for the axial interaction distance, since it is likely that the Na^+ ions bind off-axis. Furthermore, this $d_\perp$ distance does not appear to be optimal for stabilization of the cations in the binding site near the bilayer surface, but neither is it clear that optimal stabilization is desired. In fact, it is positioned such that, over the librational amplitude (shown with a heavy line), there is a maximal change in distance and hence in electrostatic influence.

The orientation of the $N_{\epsilon 1}-H$ bond and the position of these groups near the bilayer surface suggest that the tryptophans hydrogen bond to the bilayer surface. If so, these groups should be solvent accessible. Previously, in studies of these tryptophans by Raman spectroscopy, data had been interpreted to indicate that Trp_9 was not exchangeable on a time scale of a few hours (Takeuchi et al., 1990). In Figure 6, it is shown that the chemical shift resonance at 145 ppm from the oriented bilayer preparation containing $^{15}N_{\epsilon 1}$-Trp_9 is split into a 1:1:1 triplet following exposure of the hydrated (H_2O) preparation to a saturated D_2O atmosphere for 2 days at 45 °C. The exchange of ^1H for ^2H at the Trp_9 site which

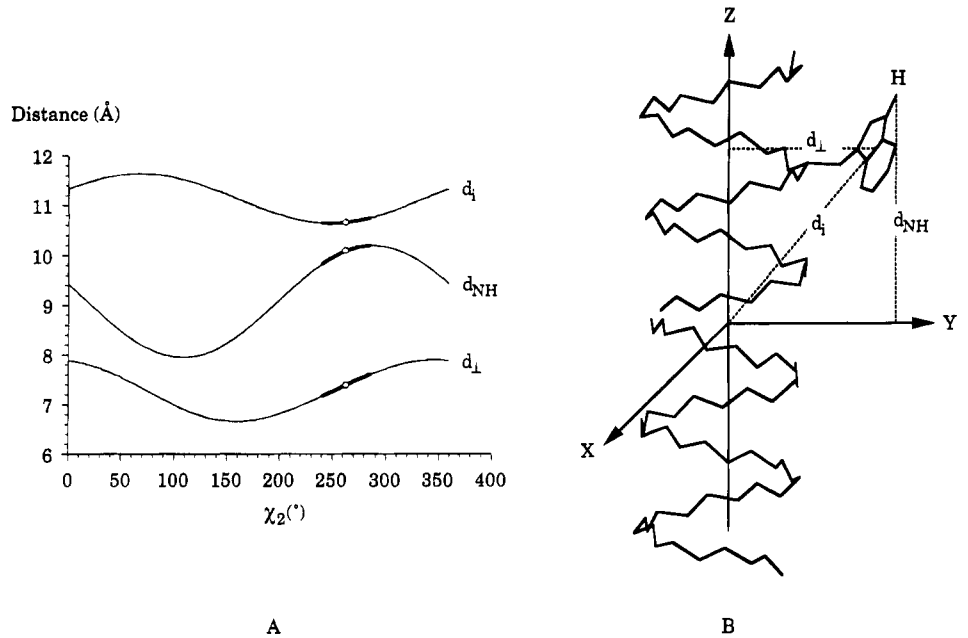

FIGURE 5: To quantitatively interpret the influence of the tryptophan side chains on function, the following distances are defined. $d_\perp$ is the distance between the dipole moment (centered on the $\delta_2-\epsilon_2$ bond in the indole ring) and the center of the helix in the *XY* plane, the plane of the lipid bilayer. d_i is defined similarly from the indole ring to the center of the channel at the bilayer center. d_{NH} is the distance between the indole NH proton to the bilayer center. For Trp_9, the χ_2 dependence on these distances at a fixed χ_1 value of 288° is shown at the left. The open circles on the curves represent the most probable value of χ_2, and the boldface lines represent the librational amplitude as determined in the accompanying paper (Hu et al., 1995). Importantly, it shows that d_i can be minimized while d_{NH} is maximized.

Table 2: ^2H Quadrupolar Splittings and Bond Orientations for Trp_{13}-d_5-Labeled Gramicidin in the Presence and Absence of Na^+ (kHz/deg)

	δ_1	ϵ_3	ζ_2	ζ_3	η_2
Trp_{13}					
with Na^+	110/36	30/130	206/165	−82/110	26/51
without Na^+	108/37	32/130	204/164	−81/110	28/51

is the most buried indole site illustrates the strong electrostatic interaction that exists between the indole and the bilayer surface and the energetic cost that would be associated with burying the indole completely within the hydrophobic domain of the bilayer.

Also shown in Figure 6 is the separated local field (SLF) experiment that correlates the $^{15}N-^1H$ dipolar interaction with the ^{15}N chemical shift. For the protonated sample, the observed dipolar interaction can be interpreted as described previously (Hu et al., 1995) to show that the bond is at an angle of 30.3° with respect to the magnetic field and the channel axis. The observed dipolar interaction from the deuterated version of the sample leads to an orientational interpretation which is within 0.9° of the SLF result. This confirms the very high accuracy as well as precision of these orientational constraints.

Before a detailed analysis of the electric dipole moments can be presented and functional implications developed, it is important to know what the influence of cations is on the indole ring orientations. Shown in Figure 7 are ^2H NMR spectra of Trp_{13}-d_5 gramicidin A in the presence and absence of Na^+. The quadrupolar splittings are tabulated in Table 2 along with the associated bond orientations for each carbon-bound deuteron. The differences are very small, suggesting that there is no significant difference in the indole ring orientations induced by the presence of Na^+. Similar results have been obtained by ^{13}C spectra (Cornell & Separovic, 1989) and by ^{15}N spectra (Ketchem et al., 1994) not only

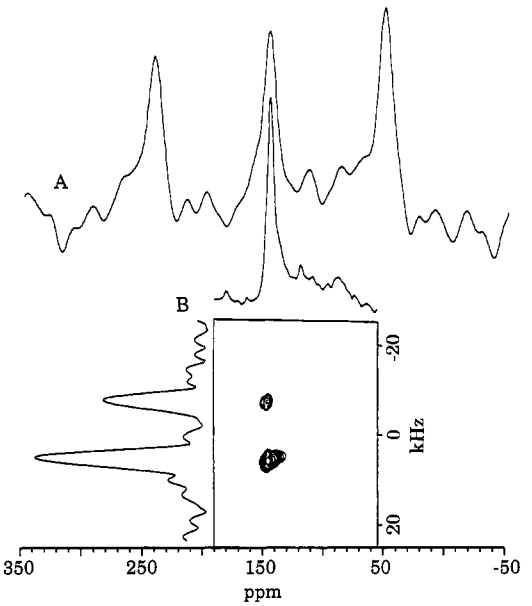

FIGURE 6: Spectra of [$^{15}N_{\epsilon 1}$-Trp_9]gramicidin A from different sample preparations in oriented lipid bilayers. (A) Deuterium exchange of the indole proton results in the observation of a triplet caused by the $^2H-^{15}N_{\epsilon 1}$ dipolar interaction between a spin $^1/_2$ and a spin 1 nucleus. The frequency separation, observed here at 20.3 MHz, of the triplet components is related to the orientation of the N−D bond with respect to the magnetic field and the channel axis which has been experimentally aligned with the field direction. The observation of the triplet shows that even Trp_9 is accessible to hydrogen exchange. (B) The triplet is compared to the chemical shift spectrum prior to the deuterium exchange where only a singlet is observed. Furthermore, a separated local field spectrum having separate axes for the chemical shift and $^1H-^{15}N$ dipolar interactions is displayed. This two-dimensional spectrum was obtained at 40.6 MHz, resulting in a doublet from the dipolar interaction between two spin $^1/_2$ nuclei which can also be interpreted to yield the orientation of the same bond measured in part A. These two data sets yield consistent results. Shown at the left is a slice through the dipolar dimension at a chemical shift of 145 ppm.

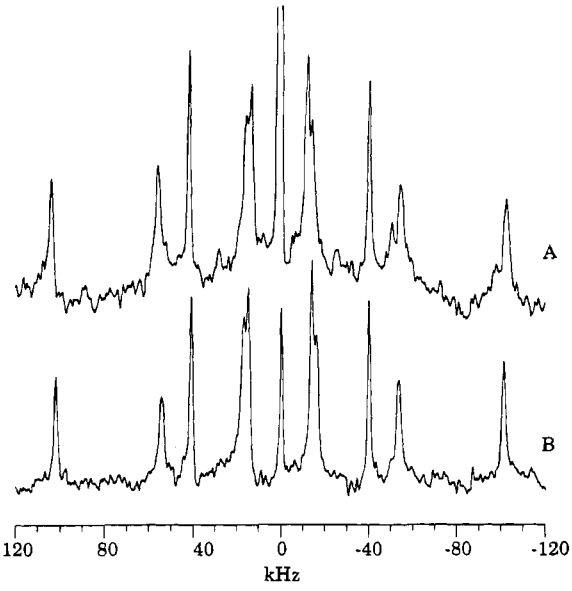

FIGURE 7: ^2H NMR spectra of Trp_{13}-d_5-labeled gramicidin A in oriented lipid bilayers (A) observed in the presence of a molar ratio of 8:1 (Na^+:gramicidin) which is equivalent to approximately 80% occupancy of the strong binding site and (B) observed in the absence of Na^+. The narrow line widths are consistent with a mosaic spread of channel axis orientations of less than ±0.3°. This remarkably high degree of alignment with respect to the magnetic field is due to alignment induced by the magnetic field through its interactions with the anisotropic diamagnetic susceptibility of the liquid crystalline array of channels.

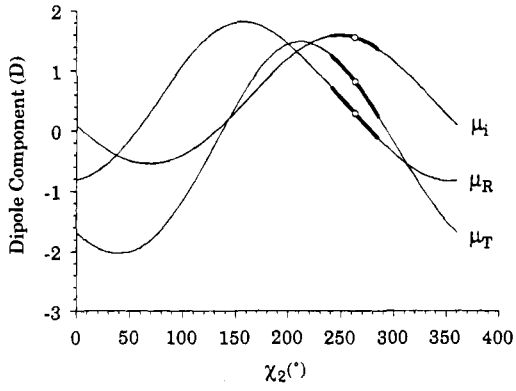

FIGURE 8: Calculated components of the indole dipole moment for the Trp_9 side chain of gramicidin as a function of the χ_2 torsion angle for a fixed χ_1 value of 288°. The open circles on the curves represent the most probable value of χ_2, and the boldface lines represent the librational amplitude as determined in the accompanying paper (Hu et al., 1995). Note that this conformation generates a maximal value for μ_i and maximal range in the value of μ_R over the librational amplitude. In fact, μ_R ranges from a value that is nonstabilizing to a value that is significantly stabilizing.

for Trp_{13} but also for all other indole sites (Hu, 1994). Therefore, the set of dipole moment components and geometric parameters presented in Table 1 obtained in the absence of Na^+ is appropriate for analyzing the influence of the indoles on conductance.

Figure 8 shows the variation of the dipole moment components for Trp_9 as a function of χ_2 (for $\chi_1 = 288°$). The radial and tangential components are calculated as well as the dipole component parallel to d_i (μ_i). In support of our conclusions from Figure 3, the most probable conformer is the one conformer that yields positive μ_i, μ_R, and μ_T components. Furthermore, it is shown that, as the indole orientation changes over its librational range, there is only a minor change in the μ_i component; however, the radial and tangential components are much more sensitive to the fluctuation in χ_2 associated with the librational range. While a stable value for μ_i is necessary for lowering the potential energy barrier at the bilayer center, such stability in μ_R and μ_T may not be necessary; in fact, instability in these parameters may result in facilitating cation translation through this channel.

DISCUSSION

A most probable conformation for each of the tryptophans has been established on the basis of functional roles of the indoles and the solid state NMR-derived orientational constraints. The torsion angles for these conformations represent minor refinements on the angles previously published (Hu et al., 1993). The set of torsion angles listed here is consistent with those described in Ketchem et al. (1993), and it is also consistent with the ±90° χ_2 torsion angles suggested for each of the tryptophans by Raman spectroscopy (Takeuchi et al., 1990). For three of the four residues, the rotameric states are the same as those determined by solution NMR in sodium dodecyl sulfate (SDS) micelles (Lomize et al., 1992). The exception is Trp_9, which in the solution NMR conformation is not stacked with Trp_{15}. Among the four possible torsional pairs described here is a stacked conformer. The argument for this conformation is twofold. First, the stacking energy is expected to be significant, and second, the tangential dipole component would have the same sign as the other tryptophan residues only if it was stacked. In SDS micelles, the hydrophobic−hydrophilic surface is curved, substantially distorting the force field that drives the indole $N_{\epsilon 1}$−H orientation to the bilayer (planar) surface (Zhang et al., 1992; Arumugam et al., 1995). Consequently, it would be expected that, if there were differences between the side chain conformations in the bilayer versus micellar structure, it would be for the more buried residues that still interact with the surface. However, recent elegant work by Koeppe and Killian (Koeppe et al., 1995) with acylated gramicidin A suggests that the Trp_9 conformation is not stacked but is similar to the conformation shown in Figure 2C. Despite these results, the arguments presented above remain strong, but we recognize the lack of a definitive structural determination for this one indole ring.

It remains somewhat unclear exactly how indoles hydrogen bond to the bilayer surface. The orientation of the lipid ester carbonyls and their distance from the bilayer center remain ambiguous in the literature. Furthermore, significant distortions in the lipid geometry may be induced by the presence of a high concentration of gramicidin. Certainly, the carbonyl groups of the ester-linked lipids remain one of the most probable hydrogen bond acceptors. In addition, the lipid head group and waters of hydration that exist at the interface are all possible acceptors. Shown here (Figure 6) is the observation that the most buried indole is solvent accessible through hydrogen exchange of the indole $N_{\epsilon 1}$−H, albeit on a time scale of 2 days at 45 °C. Exchange may be more rapid, but this lengthy time scale was necessitated by the experimental need to allow for diffusion of D_2O between the aligned bilayers of our sample.

The suggestion that the dipole moments are very important for facilitating cation transport has been supported by conductance studies on phenylalanine-substituted gramicidins

Table 3: Conductance of Gramicidin Analogs (Phe for Trp Substitutions) and the Calculated Sum of the Electrostatic Interaction Energies between the Indole Dipoles and a Cation at the Channel and Bilayer Center[a]

gramicidin analog residue no.				conductance	E_i (kJ/mol)	E_i (kJ/mol)
9	11	13	15	(pS)[b]	$\epsilon_r = 3$	$\epsilon_r = 5.1$
F	F	F	W	2.1	1.97	1.16
F	W	F	F	3.0	2.85	1.68
W	F	F	F	3.4	2.65	1.56
F	W	W	F	4.1	5.2	3.06
F	W	W	W	6.0	7.17	4.22
W	F	W	W	8.7	6.97	4.1
W	W	W	F	10.9	7.85	4.62
W	W	F	W	11.2	7.48	4.4
W	W	W	W	15.0	9.82	5.78

[a] Calculated using the most probable tryptophan side chain dihedral angles: Trp_9 (288°/263°), Trp_{11} (290°/279°), Trp_{13} (297°/270°), Trp_{15} (302°/264°). [b] The conductance data were taken from Becker et al. (1991).

(Becker et al., 1991). Because the phenylalanine side chain has no dipole moment, when it is substituted for tryptophan, the conductance rate is observed to decrease substantially. When all four phenylalanines are substituted, this effect on conductance is a factor of 20. It is possible to correlate this decrease in conductance with the increase in the rate-limiting potential energy barrier for ion transport. Using an Arrhenius equation,

$$k = A \exp[-(E_a - E_i)/RT] \quad (1)$$

where k is the conductance rate, A is a proportionality constant, E_a is the activation energy in the absence of dipole influences, and E_i is the sum of the monopole−dipole interaction energies. For a comparison of different mono-, di-, and trisubstituted (Phe for Trp) gramicidin analogs, the E_a/RT term is a constant; therefore,

$$\ln k = \ln C = A' + E_i/RT \quad (2)$$

where ln k is equated with ln C, the natural log of the measured conductance, as reported by Andersen and co-workers for the series of analogs (Becker et al., 1991; see Table 3). Furthermore, E_i can be independently calculated using the following expression for an electrostatic interaction between a monopole and a dipole and a knowledge of the high-resolution structure which yields values for μ_i and d_i

$$E_i = \mu_i e/(4\pi\epsilon_o\epsilon_r d_i^2) \quad (3)$$

where e is the charge of an electron, ϵ_o is a constant, and ϵ_r is the effective dielectric constant between the cation and the indole ring. ϵ_r is assumed to be the same for all indole−cation interaction environments.

To search for a correlation between the observed conductance measurements (ln C) and the calculated interaction energy (eq 3), two approaches have been taken. First, we have assumed a dielectric constant of 3; this is a frequently assumed value for the dielectric of the hydrocarbon region of the lipid bilayer, and it has been used previously as a reasonable estimate in similar calculations (Koeppe et al., 1990). In Figure 9A, the analysis using $\epsilon_r = 3$ is shown, while in Figure 9B, the analysis used ϵ_r as a scaling factor so that the slope of the linear relationship could be set to

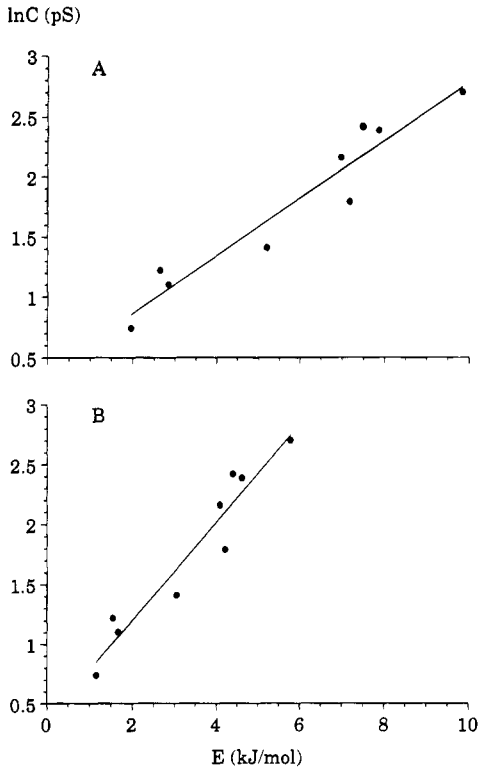

FIGURE 9: Correlations between conductance measurements and the magnitude of the monopole−dipole interaction energy. In part A, an effective dielectric constant of 3 was chosen as a reasonable dielectric for the membrane interior, while in part B, the dielectric constant was used as a scaling factor to achieve a slope of 0.41 mol/kJ ($=RT^{-1}$). The correlation between the linear least squares fit and the data is 0.96.

$(RT)^{-1}$ (Table 3). Such a slope arises when ϵ_r has a value of 5.1, a reasonable compromise between the hydrocarbon dielectric and that of a protein's interior. The correlation based on these simple energetic calculations is 0.96. This excellent correlation demonstrates that the tryptophan electric dipole is responsible for this enhancement in channel conductance and that the effect is at the monomer−monomer junction; i.e., the rate-limiting step in cation conductance is at the bilayer center.

The influence of the tangential component of the dipole on cation conductance is not interpretable without additional information describing the path for the cations through the channel. However, it is now seen how the indoles stabilize cations in the binding site on the basis of the radial components of the dipole moment. Because the path of the cation through the channel is not well-defined, the exact radial distances that should be used to calculate the energy of stabilization induced by the indoles are not easily estimated. Furthermore, the exact position of the binding site or sites is not precisely defined. However, by using the radial distances to the channel axis and a dielectric of 5.1, these interactions sum to a small time-averaged energy of stabilization (3.55 kJ/mol) that is somewhat greater than RT (2.5 kJ/mol).

As noted previously, the librational motions have only a minimal influence on the magnitude of μ_i, but there is a much greater influence on μ_R. If the four indole rings librated in unison, this would cause a change in the magnitude of the potential energy barrier of 4.2 kJ/mol ($\epsilon_r = 5.1$, Figure 10). This is calculated as a change in the electrostatic interaction

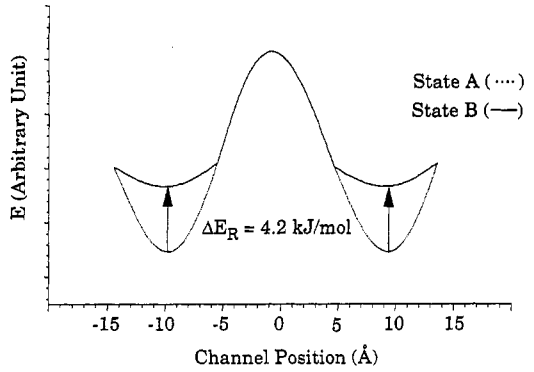

FIGURE 10: Librations significantly affect the magnitude of potential energy barrier for cation conductance. States A and B refer to the limits of the librational amplitude. The librational affect is largely through the radial components of the indole rings at the cation binding sites near the channel entrance. The magnitude of this effect has been estimated on the basis of the assumptions that the rings librate in unison and the cation is on the channel axis. The former assumption is likely to be only partially true, thereby reducing the magnitude of this effect. However, the cations are likely to bind off-axis, thereby increasing this effect.

energy for the μ_R components between the limits of their librational range and for the cation on the channel axis adjacent to the indole rings. Such correlated motions would be unlikely for all four indoles, but quite reasonable for Trp_9 and Trp_{15}. In addition, if the cation traverses the channel off-axis, the energy fluctuation induced by individual indoles would be more significant. It is possible that such fluctuations could form a rapid gate for conductance by raising the energy in the binding site to destabilize the cation and promote its passage through the channel. Preliminary relaxation results indicate that the librational motions are on the nanosecond or near nanosecond time scale (W. Hu, F. Tian, and T. A. Cross, unpublished results), consistent with the translational kinetic time scale of 10 ns (Andersen, 1983; Roux & Karplus, 1991; Becker et al., 1992). It has recently been reported that this kinetic time scale is coincident with librational motions in the polypeptide backbone that occur about the $C_\alpha-C_\alpha$ axis (North & Cross, 1995).

These functional roles for tryptophan illustrated in gramicidin are undoubtedly reproduced in many membrane proteins, where it is known that the tryptophan amino acid content is much greater than in water soluble proteins. Furthermore, it has been shown for several membrane proteins that the indoles are oriented much like they are in gramicidin with their $N_{\epsilon 1}-H$ positioned for hydrogen bonding to the surface (Michel & Deisenhofer, 1990; Henderson et al., 1990; Meers, 1990; Chattopadhyay & McNamee, 1991; Schiffer et al., 1992). These hydrogen bonds help to align proteins with respect to the bilayer plane for optimal functional activity. The functional utilization of the dipoles has not been documented for other membrane proteins, but there are many such proteins from ion channels to electron transport proteins that could be facilitated by the optimal orientation of indole rings. In fact, for the photosynthetic reaction center, a dielectric asymmetry has recently been described to distinguish between the two nearly equivalent potential electron transfer pathways (Steffen et al., 1994). To gain such functional understanding of macromolecular systems, it is necessary to achieve high-resolution structural and dynamic characterizations. The paucity of such information is due to the difficulty of crystallizing these proteins or solubilizing native conformations in isotropic solution. However, solid state NMR of such proteins in anisotropic environments is demonstrated here and elsewhere as a viable approach for obtaining both high-resolution structure and dynamics.

ACKNOWLEDGMENT

We are deeply indebted to the staff of the FSU NMR Facility, J. Vaughn, R. Rosanske, and T. Gedris, for their skillful maintenance of the facility and spectrometers and to the staff of the Bioanalytical Synthesis and Services Facility, H. Henricks and U. Goli, for their expertise and maintenance of the ABI 430A peptide synthesizer and HPLC equipment.

REFERENCES

Andersen, O. S. (1983) *Biophys. J. 41*, 119−133.
Arumugam, S., Pascal, S., North, C. L., Hu, W., Lee, K.-C., Cotten, M., Ketchem, R. R., Xu, F., Brenneman, M., Kovacs, F., Tian, F., Wang, A., Huo, S., & Cross, T. A. (1995) *Proc. Natl. Acad. Sci. U.S.A.* (submitted for publication).
Becker, M. D., Greathouse, D. V., Koeppe, R. E., II, & Andersen, O. S. (1991) *Biochemistry 30*, 8830−8839.
Becker, M. D., Koeppe, R. E., II, & Andersen, O. S. (1992) *Biophys. J. 62*, 25−27.
Benamar, D., Daumas, P., Trudelle, Y., Calas, B., Bennes, R., & Heitz, F. (1993) *Eur. Biophys. J. 22*, 145−150.
Burley, S. K., & Petsko, G. A. (1985) *Science 229*, 23−28.
Busath, D. (1993) *Annu. Rev. Physiol. 55*, 473−501.
Chattopadhyay, A., & McNamee, M. G. (1991) *Biochemistry 30*, 7159−7164.
Cross, T. A. (1994) *Annu. Rep. NMR Spectrosc. 29*, 123−167.
Cross, T. A., & Opella, S. J. (1994) *Curr. Opin. Struct. Biol. 4*, 574−581.
Daumas, P., Benamar, D., Heitz, F., Ranjalahy-Rasoloarijao, L., Mouden, R., Lazaro, R., & Pullman, A. (1991) *Int. J. Pept. Protein Res. 38*, 218−228.
Elber, R., Chen, D. P., Rojewska, D., & Eisenberg, R. (1995) *Biophys. J. 68*, 906−924.
Henderson, R., Baldwin, J. M., Ceska, T. A., Zemlin, F., Beckmann, E., & Downing, K. H. (1990) *J. Mol. Biol. 213*, 899−929.
Hinton, J. F., Fernandez, J. Q., Shungu, D. C., Whaley, W. L., Koeppe, R. E., II, & Millet, F. S. (1988) *Biophys. J. 54*, 527−533.
Hladky, S. B., Urban, B. W., & Haydon, D. A. (1979) in *Ion Permeation Membrane Channels* (Steven, C. F., & Tsien, R. W., Eds.) pp 89−104, Raven Press, New York.
Hu, W. (1994) Ph.D. Dissertation, Florida State University, Tallahassee, FL.
Hu, W., Lee, K.-C., & Cross, T. A. (1993) *Biochemistry 32*, 7035−7047.
Hu, W., Lazo, N. D., & Cross, T. A. (1995) *Biochemistry 34*, 14138−14146.
Jordan, P. C. (1990) *Biophys. J. 58*, 1133−1156.
Ketchem, R. R., Hu, W., & Cross, T. A. (1993) *Science 261*, 1457−1460.
Ketchem, R. R., Hu, W., Tian, F., & Cross, T. A. (1994) *Structure 2*, 699−701.
Killian, J. A. (1992) *Biochim. Biophys. Acta 1113*, 391−425.
Koeppe, R. E., II, Mazet, J.-L., & Andersen, O. S. (1990) *Biochemistry 29*, 512−520.
Koeppe, R. E., II, Killian, J. A., & Greathouse, D. V. (1994) *Biophys. J. 66*, 14−24.
Koeppe, R. E., II, Killian, J. A., Vogt, T. C. B., de Kruijff, B., Taylor, M. J., Mattice, G. L., & Greathouse, D. V. (1995) *Biochemistry 34*, 9299−9306.
Lazo, N. D., Hu, W., & Cross, T. A. (1992) *J. Chem. Soc., Chem. Commun.*, 1529−1531.
Lee, K.-C., Huo, S., & Cross, T. A. (1995) *Biochemistry 34*, 857−867.
Lomize, A. L., Orechov, V. Yu., & Arseniev, A. S. (1992) *Bioorg. Khim. 18*, 182−200.
Meers, P. (1990) *Biochemistry 29*, 3325−3330.

Meulendijks, G. H. W. M., Sonderkamp, T., Dubois, J. E., Nielen, R. J., Kremers, J. A., & Buck, H. M. (1989) *Biochim. Biophys. Acta 979*, 321−330.
Michel, M., & Deisenhofer, J. (1990) *Curr. Top. Membr. Transp. 36*, 53−69.
North, C. L., & Cross, T. A. (1995) *Biochemistry 34*, 5883−5895.
O'Connell, A. M., Koeppe, R. E., II, & Andersen, O. S. (1990) *Science 250*, 1256−1259.
Roux, B., & Karplus, M. (1991) *J. Phys. Chem. 95*, 4856−4868.
Scarlatta, S. F. (1988) *Biophys. J. 54*, 1149−1157.
Scarlatta, S. F. (1991) *Biochemistry 30*, 9853−9859.
Schiffer, M., Chang, C.-H., & Stevens, F. J. (1992) *Protein Eng. 5*, 213−214.
Seoh, S.-A., & Busath, D. (1995) *Biophys. J. 68*, 2271−2279.
Separovic, F., & Cornell, B. A. (1989) *Biophys. J. 55*, 504a.
Separovic, F., Hayamizu, K., Smith, R., & Cornell, B. A. (1991) *Chem. Phys. Lett. 181*, 157−162.
Skerra, A., & Brickmann, J. (1987) *Biophys. J. 51*, 969−976.
Steffen, M. A., Lao, K., & Boxer, S. G. (1994) *Science 264*, 810−816.
Takeuchi, H., Nemoto, Y., & Harada, I. (1990) *Biochemistry 29*, 1572−1579.
Tredgold, R. H., Hole, P. N., & Sproule, R. C. (1977) *Biochim. Biophys. Acta 471*, 189−194.
Urry, D. W., Trapane, T. L., Walker, J. T., & Prasad, K. U. (1982) *J. Biol. Chem. 257*, 6659−6661.
Urry, D. W., Trapane, T. L., Venkatachalam, C. M., & McMichens, R. B. (1989) *Methods Enzymol. 171*, 286−342.
Van Mau, N., Trudelle, Y., Daumas, P., & Heitz, F. (1988) *Biophys. J. 54*, 563−567.
Van Mau, N., Bonnet, B., Benayad, A., & Heitz, F. (1994) *Eur. Biophys. J. 22*, 447−452.
Weiler-Feischenfeld, H., Pullman, A., Berthod, H., & Giessner-Prettre, C. (1970) *J. Mol. Struct. 6*, 297−304.
Zhang, Z., Pascal, S. M., & Cross, T. A. (1992) *Biochemistry 31*, 8822−8828.

BI951625Q